Chemical and Photochemical Water Oxidation Catalyzed by Mononuclear Ruthenium Complexes with a Negatively Charged Tridentate Ligand

6 AUTHORS, INCLUDING:

Lele Duan
KTH Royal Institute of Technology
36 PUBLICATIONS **1,627** CITATIONS

SEE PROFILE

Xu Yunhua
KTH Royal Institute of Technology
34 PUBLICATIONS **1,514** CITATIONS

SEE PROFILE

Mikhail Gorlov
KTH Royal Institute of Technology
39 PUBLICATIONS **1,041** CITATIONS

SEE PROFILE

Samir Andersson
KTH Royal Institute of Technology
10 PUBLICATIONS **270** CITATIONS

SEE PROFILE

Chemical and Photochemical Water Oxidation Catalyzed by Mononuclear Ruthenium Complexes with a Negatively Charged Tridentate Ligand

Lele Duan,[a] Yunhua Xu,[a] Mikhail Gorlov,[a] Lianpeng Tong,[a] Samir Andersson,[a] and Licheng Sun*[a, b]

Abstract: Two mononuclear ruthenium complexes [RuL(pic)$_3$] (**1**) and [RuL-(bpy)(pic)] (**2**) (H$_2$L = 2,6-pyridinedicarboxylic acid, pic = 4-picoline, bpy = 2,2′-bipyridine) have been synthesized and fully characterized. Both complexes could promote water oxidation chemically and photochemically. Compared with other known ruthenium-based water oxidation catalysts using [Ce(NH$_4$)$_2$(NO$_3$)$_6$] (Ce^{IV}) as the oxidant in solution at pH 1.0, complex **1** is one of the most active catalysts yet reported with an initial rate of 0.23 turnover s^{-1}. Under acidic conditions, the equatorial 4-picoline in complex **1** dissociates first. In addition, ligand exchange in **1** occurs when the Ru^{III} state is reached. Based on the above observations and MS measurements of the intermediates during water oxidation by **1** using Ce^{IV} as oxidant, [RuL(pic)$_2$(H$_2$O)]$^+$ is proposed as the real water oxidation catalyst.

Keywords: electrochemistry · homogeneous catalysis · oxidation · ruthenium · water splitting

Introduction

The oxygen-evolving complex (OEC) in photosystem II, which can oxidize water into molecular oxygen, is one of the most remarkable inventions of nature. With this system, green plants and other photosynthetic organisms can convert the photoenergy of sunlight into chemical energy. Recent X-ray crystallographic studies have revealed that the OEC contains a Mn$_4$O$_x$Ca cluster and it is this species that plays the active role in water oxidation.[1–4] Artificial systems performing similar functions as the OEC have attracted great attention in the past few years due to the increase in demand for solar energy conversion.[5–8] Light-driven water oxidation or water splitting has been demonstrated by the direct electrolysis of water by photovoltaic cells,[9] semiconductor-based photoelectrodes,[10–13] and catalytic systems composed of transition-metal photosensitizers and metal oxide water oxidation catalysts.[14,15] In contrast, light-driven water oxidation by molecular catalysts has rarely been reported, mainly due to the lack of suitable catalysts bearing a low overpotential for water oxidation.

Although considerable effort has been directed towards mimicking the structure of OEC, only a few synthetic manganese complexes so far have achieved water oxidation with modest catalytic activity.[16–20] On the other hand, by using other transition metals (ruthenium or iridium) instead of manganese, significant improvements have been made in homogeneously catalyzed water oxidation. Since Meyer and co-workers reported an oxo-bridged dinuclear ruthenium complex, {cis,cis-[Ru(bpy)$_2$(H$_2$O)]$_2$(μ-O)}$^{4+}$, the so-called "blue dimer", that efficiently catalyzes water oxidation,[21,22] several derivatives of the blue dimer have been synthesized with more or less enhanced catalytic activities.[23–26] A series of amine-coordinated ruthenium complexes, [(NH$_3$)$_5$Ru^{III}(μ-O)Ru^{IV}(NH$_3$)$_4$(μ-O)Ru^{III}(NH$_3$)$_5$]$^{6+}$, for instance, were investigated as water oxidation catalysts by Yagi and Kaneko in both homogenous and heterogeneous systems.[27] A few years ago, Llobet and Tanaka and their co-workers, respectively, reported {[Ru^{II}(terpy)(H$_2$O)]$_2$(μ-bpp)}$^{3+}$ (bpp = 2,6-bis(pyridyl)pyrazolate) and [Ru$_2$(OH)$_2$(3,6-Bu$_2$Q)$_2$(btpyan)]-(SbF$_6$)$_2$ (3,6-Bu$_2$Q = 3,6-di-tert-butyl-1,2-benzoquinone; btpyan = 1,8-bis(2,2′:6′,2″-terpyridyl-4′-yl)anthracene).[28,29]

[a] L. Duan, Dr. Y. Xu, Dr. M. Gorlov, L. Tong, S. Andersson,
Prof. L. Sun
Department of Chemistry, Royal Institute of Technology (KTH)
Teknikringen 30, 10044 Stockholm (Sweden)

[b] Prof. L. Sun
DUT-KTH Joint Education and Research Center
on Molecular Devices
State Key Laboratory of Fine Chemicals
Dalian University of Technology (DUT)
116012 Dalian (China)
Fax: (+46) 8-7912333
E-mail: lichengs@kth.se

Meyer and Sakai and their co-workers recently reported several mononuclear ruthenium aqua complexes containing terpyridine as the backbone with only one aqua ligand in each complex,[30,31] and Meyer and co-workers proposed the formation of a seven-coordinated ruthenium intermediate during the catalytic process.[30] Thummel and co-workers developed a series of nonaqueous ruthenium-based water oxidation catalysts with high reactivity and proposed a tentative mechanism also involving a seven-coordinated ruthenium species.[32–35] To avoid using organic ligands in the construction of water oxidation catalysts, Hill and Bonchio and their co-workers independently developed a new purely inorganic water-soluble catalyst, a ruthenium polyoxometalate $[\{Ru_4O_4(OH)_2(H_2O)_4\}(\gamma\text{-}SiW_{10}O_{36})_2]^{10-}$.[36,37] Although ruthenium-based complexes have shown promising catalytic properties towards water oxidation, one of their disadvantages is their lack of robustness. Bernhard and co-workers recently reported a series of robust iridium catalysts that are capable of catalyzing water oxidation over several days but with low reaction rates.[38] To increase the activity of the iridium catalysts, Crabtree and co-workers designed several Cp*-based (Cp* = C_5Me_5) iridium complexes with an electron-donating ligand that had higher reaction rates and reduced robustness.[39]

For light-driven water oxidation by molecular catalysts, to date, only a couple of dimeric ruthenium complexes,[40,41] a tetraruthenium polyoxometalate complex,[42] two ruthenium nonaqueous complexes with negatively charged ligands (complexes **a** and **b** in Scheme 1),[43,44] and $CoSO_4$[45] have

been reported to promote photochemical water oxidation in the presence of a ruthenium-based polypyridyl photosensitizer and sacrificial electron acceptor (see Figure 1 for an illustration of the principle). In addition, Milstein and co-workers have reported a Ru^{II} complex that splits water stoichiometrically into dihydrogen and dioxygen in consecutive thermal and light-driven steps.[46]
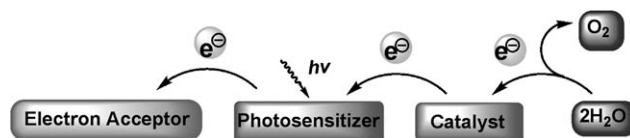

Figure 1. Visible-light-driven water oxidation by means of a three-component molecular system.

With a view to light-driven water oxidation, we attempted to lower the oxidation potential of ruthenium-based water oxidation catalysts by introducing negatively charged ligands.[47,48] Owing to the strong electron-donating ability of the negatively charged ligand, a seven-coordinated Ru^{IV} intermediate has successfully been isolated and characterized by X-ray diffraction.[48] Because mononuclear ruthenium complexes with terpyridine as a backbone can catalyze water oxidation with high turnover numbers (TONs),[30,31,33] we were motivated to synthesize mononuclear ruthenium complexes with a negatively charged tridentate ligand, 2,6-pyridinedicarboxylate. The negatively charged ligand can increase the electron density of the ruthenium center and thus lower the oxidation potential, which makes it possible to match the oxidation potential of the catalyst with that of commonly used photosensitizers. Herein, we present two mononuclear ruthenium complexes $[RuL(pic)_3]$ (**1**) and $[RuL(bpy)(pic)]$ (**2**) (H_2L = 2,6-pyridinedicarboxylic acid, pic = 4-picoline, bpy = 2,2′-bipyridine; Scheme 1) and describe their preparation, spectroscopic characterization, electrochemical properties, and chemical and photochemical water oxidation performances.

Results and Discussion

Synthesis and characterization: Heating a mixture of H_2L, $[Ru(dmso)_4Cl_2]$, and triethylamine in acetonitrile at reflux overnight followed by the addition of 4-picoline afforded **1** in an isolated yield of 72%. For the preparation of complex **2**, a similar procedure was used: Reaction of H_2L, $[Ru(dmso)_4Cl_2]$, and bipyridine gave the $[RuL(bpy)Cl]^-$ species, which was proved by MS but not isolated. 4-Picoline was added to the above intermediate solution to give the final product **2** in an isolated yield of 56%.

Complexes **1** and **2** were characterized by ^1H NMR, IR, and UV/Vis spectroscopies and elemental analysis. In addition, the structure of complex **1** was confirmed by X-ray diffraction. The ^1H NMR spectra of these two complexes showed well-resolved peaks, for example, the ^1H NMR spec-
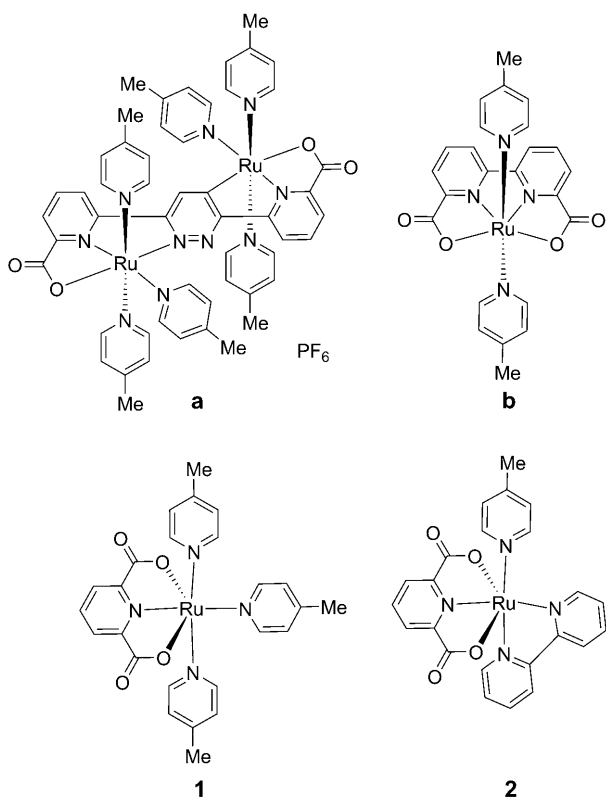
Scheme 1. Molecular structures of **a**, **b**, **1**, and **2**.

trum of **1** in CDCl$_3$ shows 15 proton resonances in the aromatic region and 9 proton resonances in the upfield region. The doublet at $\delta = 7.95$ ppm and triplet at $\delta = 7.54$ ppm are from ligand L^{2-}. The signals at $\delta = 8.75$, 8.12, 7.06, and 6.87 ppm have been assigned to the aromatic ring protons of the 4-picoline ligands. The signals at $\delta = 2.35$ and 2.22 ppm, observed in a ratio of 1:2, arise from the methyl protons of the equatorial and axial 4-picolines, respectively. These signals indicate the symmetric nature of complex **1**, which is consistent with the proposed structure.

The IR spectra of **1** and **2** display two strong bands in the carbonyl region of 1618–1646 cm^{-1}. It is noticeable that the frequency of the first CO band of complex **2** is higher than that of complex **1**. Introduction of 4-picoline, which is a good electron donor, causes the C=O bands of complex **1** to shift to a lower wavelength.

The electronic absorption spectra of these two complexes in CH$_3$CN at room temperature display very intense bands in the near-UV region of 200–300 nm. These are assigned to π–π* transitions in the ligands. The weaker and lower-energy bands in the visible region are attributable to a series of metal-to-ligand charge-transfer (MLCT) bands. It is clear that complex **2** shows lower-energy MLCT bands than complex **1**, possibly due to a low-lying π* orbital (LUMO) in the bpy ligand in complex **2**.

The X-ray crystal structure of complex **1** is represented in Figure 2. There are two independent ruthenium molecules and five solvate water molecules in the unit cell of the crystal. Significant interatomic distances and angles are listed in Table 1. The ruthenium atoms have distorted octahedral co-

Table 1. Selected bond lengths [Å] and angles [°] for the two molecules in the unit cell of the crystal of **1**.

Molecule 1		Molecule 2	
Ru1–N1	2.068(6)	Ru2–N5	2.083(6)
Ru1–N2	2.078(6)	Ru2–N6	2.097(6)
Ru1–N3	2.092(6)	Ru2–N7	2.093(6)
Ru1–N4	1.947(6)	Ru2–N8	1.943(6)
Ru1–O1	2.119(5)	Ru2–O5	2.137(5)
Ru1–O3	2.146(5)	Ru2–O7	2.126(5)
N1-Ru1-N3	174.7(2)	N8-Ru2-O5	79.0(2)
N2-Ru1-O1	100.6(2)	N6-Ru2-O5	100.9(2)
N4-Ru1-O1	79.3(2)	N6-Ru2-O7	101.1(2)
N4-Ru1-O3	78.7(2)	N5-Ru2-N7	176.2(2)
N1-Ru1-N4	92.7(2)	N5-Ru2-O5	91.2(2)
N1-Ru1-N2	84.5(2)	N5-Ru2-O7	88.1(2)
N3-Ru1-O1	88.6(2)	N6-Ru2-N7	86.7(2)
N3-Ru1-O3	91.1(2)	N7-Ru2-N8	92.0(2)
O1-Ru1-O3	158.0(2)	O5-Ru2-O7	158.0(2)

ordination: The O-Ru-O angle is 158.0(2)°. The Ru–N distances lie in the range 1.9–2.1 Å; the Ru–N(4-picoline) distances are slightly longer than those between ruthenium and the nitrogen atoms belonging to ligand L^{2-}. The chelating ligand L^{2-} has an almost planar structure. The water molecules form hydrogen bonds with the carboxylato groups; the shortest O2–O12 distance is 2.90(2) Å.

Labile carboxylate ligation: The carboxylate ligation in complexes **1** and **2** is labile in aqueous solution. In D$_2$O/CD$_3$CN (4:1, v/v), three ^{1}H NMR peaks arising from ligand L^{2-} were observed for both **1** and **2** (see Figures S1 and S2 in the Supporting Information). However, no release of 4-picoline was observed. The change in the ^{1}H NMR spectra of complexes **1** and/or **2** in aqueous solution is most likely due to the dissociation of one carboxylate ligand from the ruthenium atom and subsequent ligation of the solvent to the metal center. The MS spectra of complexes **1** and **2** in H$_2$O/CH$_3$CN (4:1, v/v) show two peaks at m/z 587.7 and 557.8, respectively, assigned to the monocationic species [**1**–S+H]$^+$ (calculated value: 588.12) and [**2**–S+H]$^+$ (calculated value: 558.07), which indicates that it is acetonitrile that replaces one of the carboxylate ligands. The structures of **1**–S and **2**–S are shown in Scheme 2.

Electrochemistry of complexes 1 and 2: As potential water oxidation catalysts, the redox properties of the model complexes are among their most interesting features. Therefore, the electrochemical properties of these two complexes were investigated in different solvents.

Complexes **1** and **2** in dichloromethane show one reversible redox couple with $E_{1/2}$ values of 0.51 and 0.60 V versus NHE, respectively, which were assigned to the Ru$^{II/III}$ redox process (see cyclic voltammograms (CVs) in Figure S3; in organic solvents, potentials versus NHE were converted by assuming that the $E_{1/2}$ value of the Fc$^+$/Fc redox couple is 0.63 V vs. NHE; in aqueous solution, [Ru(bpy)$_3$]$^{2+}$ was used as a reference with $E_{1/2}$(Ru$^{II/III}$) = 1.26 V vs. NHE).
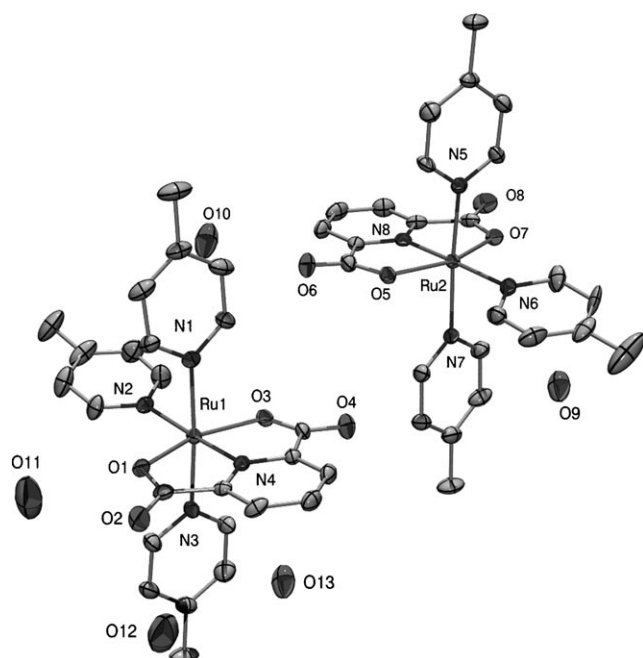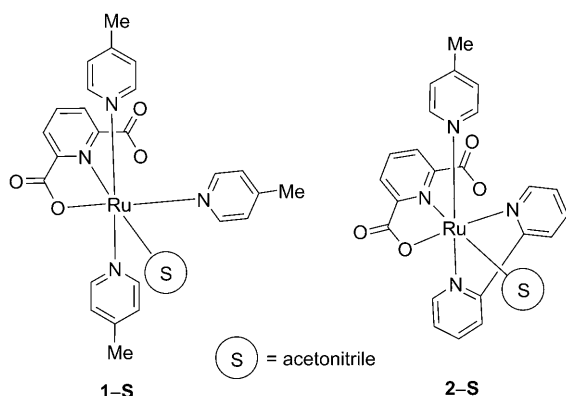

Figure 2. The X-ray crystal structure of complex **1** with thermal ellipsoids at the 50% probability level (hydrogen atoms have been omitted for clarity). The oxygen atoms O9, O10, O11, and O12 are from solvate water molecules.

Scheme 2. Structures of **1–S** and **2–S**.

Note again that complex **1** in H_2O/CH_3CN leads to **1–S**. In an aqueous solution containing 10% acetonitrile at pH 1.0 and at a scan rate of 100 mV s^{-1} (Figure 3, lower),
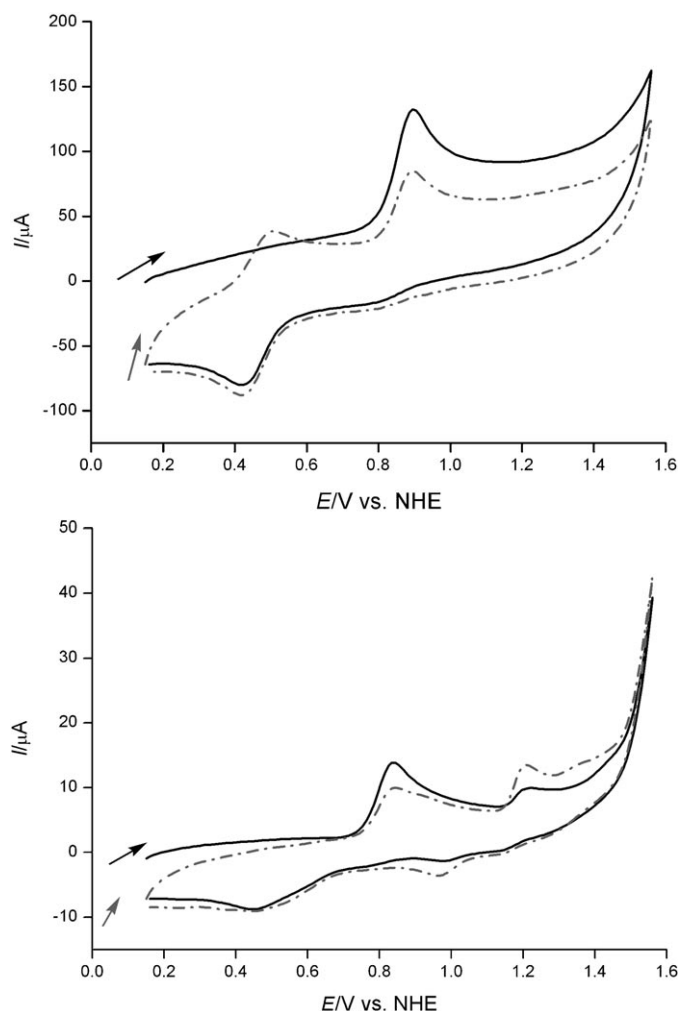



Figure 3. CVs of complex **1** in aqueous solution (pH 1.0) containing 10% acetonitrile at scan rates of 5000 (upper) and 100 mV s^{-1} (lower). ——: first scan, –·–·: second scan.

compound **1–S** shows an irreversible oxidation peak at 0.84 V relative to the Ru$^{II/III}$ process, which indicates that a chemical reaction occurs when the Ru^{III} state is reached. A further scan in the cathodic direction gives a small peak at 1.21 V and repeated scans lead to a decrease in the first oxidation peak and an increase in the second. Two reduction peaks at 0.97 and 0.46 V (weak, broad, and irreversible) were detected in the reverse scan. At a higher scan rate (5000 mV s^{-1}), the oxidation peak at 0.84 V was still irreversible, the aforementioned oxidation peak at 1.21 V disappeared, and the reduction peak at 0.46 V became sharp and reversible (Figure 3, upper). The new couple at 0.46 V was tentatively assigned to the Ru$^{II/III}$ redox process related to complex **1** because the redox potential is close to the $E_{1/2}$-(Ru$^{II/III}$) value of complex **1** observed in CH_2Cl_2. Therefore, the first chemical reaction following the oxidation of **1–S** is the formation of [Ru^{III}L(pic)$_3$]. [Ru^{III}L(pic)$_3$] is not stable because the peak at 0.46 V becomes weak and broad at the low scan rate. It undergoes dissociation of 4-picoline (see below). In addition, a catalytic curve was found starting at 1.53 V. According to the irreversibility of the redox peaks, as a reactive precursor, complex **1** undergoes ligand exchange to produce an active species for water oxidation. Similarly to complex **1**, complex **2** in aqueous solution containing 10% acetonitrile produces complex **2–S** (Scheme 2). The CVs of complex **2–S** at different scan rates (100 mV s^{-1} to 40 V s^{-1}) are presented in Figure S4 in the Supporting Information. The onset potential of the catalytic curve was found at around 1.46 V. The electrochemical properties of complex **1** in an aqueous solution containing 10% acetonitrile at pH 1.0 are summarized in Scheme 3.

To prove that [Ru^{III}L(pic)$_3$] undergoes 4-picoline dissociation in aqueous solution, complex **1** was chemically oxidized with 1.1 equiv of tris(4-bromophenyl)ammonium hexachloroantimonate ($E = 1.07$ V vs. NHE in CH_3CN)[49] in CD_3CN followed by the addition of D_2O and the resulting solution after filtration was analyzed by ^{1}H NMR spectroscopy, which showed the formation of free 4-picoline. This result suggests that [Ru^{III}L(pic)$_3$]$^+$ in aqueous solution undergoes 4-picoline dissociation, which provides a free site for water to coordinate. For comparison, complex **2** was treated in a similar way, however, no free 4-picoline was detected.

The redox properties of **1** and **2** in pH 7.0 phosphate buffer containing 10% acetonitrile were also investigated and of course **1–S** and **2–S** were the dominating species (see the CVs in Figures S5 and S6 in the Supporting Information). At a scan rate of 100 mV s^{-1}, two irreversible peaks were detected for each complex in the first scan and the onset potentials of the catalytic curves were observed at 1.26 and 1.32 V for solutions of complexes **1** and **2**, respectively. The complexity of the CVs observed in pH 7.0 phosphate buffer solution prevents us interpreting the mechanisms. Notably, the onset potentials of the catalytic curves for aqueous solutions of complexes **1** and **2** are 120 and 60 mV, respectively, lower than the $E_{1/2}$(Ru$^{II/III}$) value of [Ru(bpy)$_2$(dcb)]$^{2+}$ (dcb = 4,4′-dicarboxyethyl-2,2′-bipyridine; $E_{1/2}$(Ru$^{II/III}$) = 1.38 V vs. NHE), which means that [Ru(bpy)$_2$-
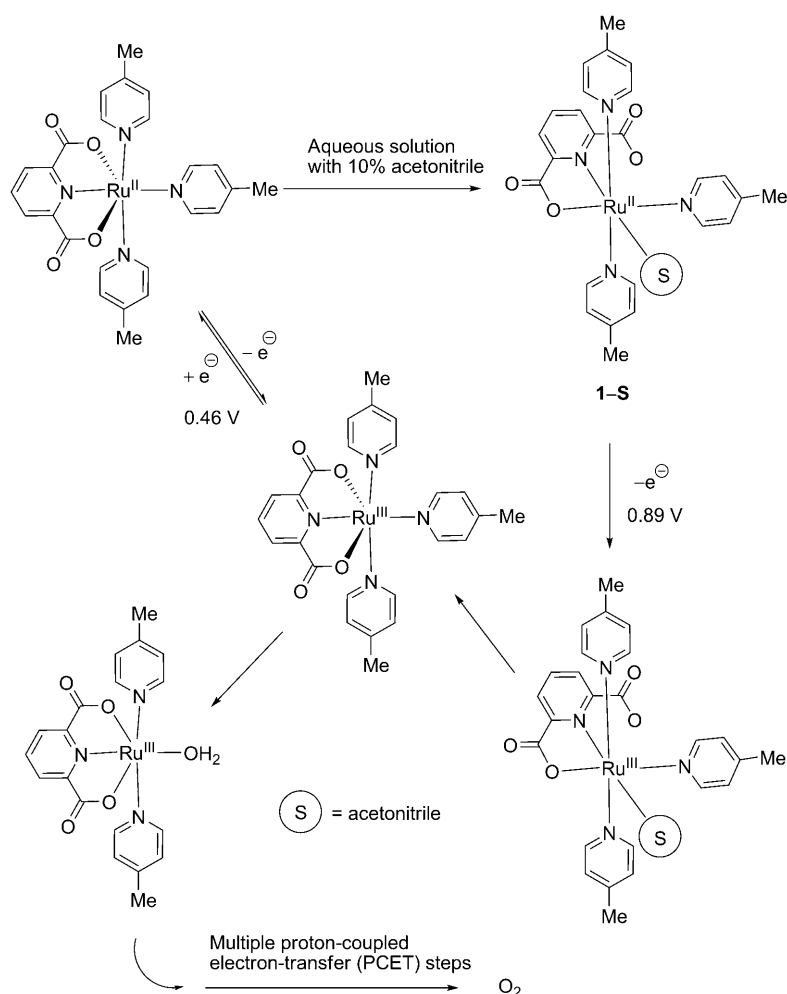
Scheme 3. Proposed mechanism for complexes **1** in aqueous solution (pH = 1.0, adjusted by CF$_3$SO$_3$H) containing 10% acetonitrile.

ing protonation of 4-picoline. The intensity of this new peak increased considerably after 12 h (Figure 4e), which means that a large amount of 4-picoline in complex **1** is protonated under the acidic conditions and released from the ruthenium center, and that a solvent molecule might coordinate to the ruthenium ion in the meantime. In addition, it is clear that the new complex is also symmetric because it shows only one CH$_3$ resonance at $\delta = 2.40$ ppm. Accordingly, the first ligand to be released under acidic conditions is the equatorial 4-picoline. Otherwise the new complex would show two CH$_3$ resonances. In contrast, no dissociation of 4-picoline was observed with complex **2** under the same conditions. Thus, dissociation of 4-picoline is much easier in complex **1** than in complex **2** under acidic conditions. This is probably one of the reasons why complex **1** shows much better activity in water oxidation than complex **2** (see below).

(dcb)]$^{3+}$ could potentially drive precatalysts **1** and **2** to oxidize water in pH 7.0 phosphate buffer.

Protonation study: To test the stabilities of our complexes in acidic conditions, we investigated the protonation properties of complexes **1** and **2** with CF$_3$SO$_3$H to see whether 4-picoline could be released and a water molecule coordinated to the ruthenium ion.

Protonation studies of 4-picoline and complex **1** were carried out by ^{1}H NMR spectroscopy in D$_2$O/CD$_3$CN (4:1, v/v). The signals in Figure 4a ($\delta = 2.40$ ppm) and Figure 4c ($\delta = 2.34$ and 2.42 ppm) represent the proton resonances of the CH$_3$ groups of free 4-picoline and complex **1**, respectively. When a large excess of CF$_3$SO$_3$H was added to the solution of 4-picoline, the singlet of the CH$_3$ group at $\delta = 2.40$ ppm (Figure 4a) was shifted downfield by 0.29 ppm and the new singlet at $\delta = 2.69$ ppm (Figure 4b) was assigned to the CH$_3$ group of the protonated 4-picoline. After the addition of the same equivalents of CF$_3$SO$_3$H to complex **1**, a small new peak at $\delta = 2.68$ ppm appeared (Figure 4d), which is in agreement with the chemical shift of the CH$_3$ group follow-

Chemical water oxidation: Chemical water oxidation was demonstrated by using Ce^{IV} as an oxidant in an aqueous solution at pH 1.0. The formation of oxygen was measured with an oxygen sensor and the amount of oxygen generated was calibrated by GC. Both **1** and **2** are active towards water oxidation. When a solution of complex **1** in acetonitrile was added to an aqueous solution of CF$_3$SO$_3$H (pH 1.0) containing excess Ce^{IV}, a strong response was observed from the oxygen sensor (Figure 5), which indicates a high catalytic activity in water oxidation. The TON was calculated to be 550 with an initial rate of 0.23 turnover s^{-1}, which are comparable to the values determined with Thummel's ruthenium catalysts.[33] For complex **2**, a low turnover number of 17 was found with an initial rate of 0.0072 turnovers^{-1}. For comparison, the catalytic properties of two known ruthenium-based water oxidation catalysts, [Ru(tpy)(pynap)Cl]$^+$ (**3**; tpy = 2,2':6',2''-terpyridine; pynap = 2-(2'-pyridyl)-1,8-naphthyridine) and [Ru-(tpy)(pic)$_3$]$^{2+}$ (**4**), are summarized together with those of complexes **1** and **2** in Table 2.[33] The data shows that complex **1** has a higher reaction rate than complex **3**, which has recently been reported as a highly active water oxidation catalyst. However, the lack of robustness of **1** leads to a
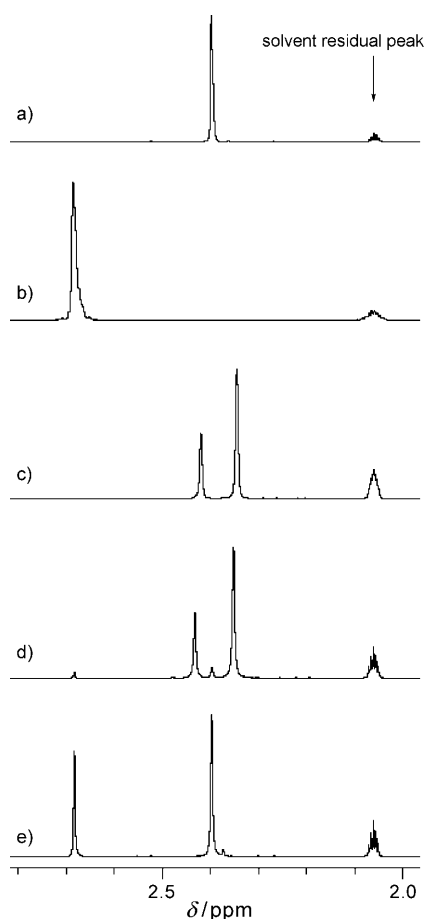
Figure 4. ^{1}H NMR spectra in D_2O/CD_3CN (4:1, v/v) of a) 4-picoline, b) 4-piconline and 70 equiv CF_3SO_3H, c) complex **1**, d) complex **1** and 70 equiv CF_3SO_3H, and e) complex **1** and 70 equiv CF_3SO_3H (12 h later).
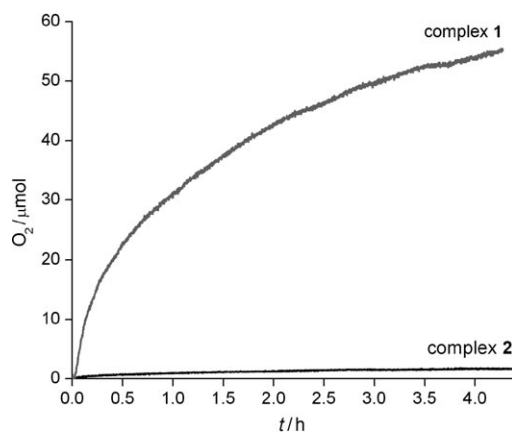

Figure 5. Evolution of oxygen recorded in the gas phase with an oxygen sensor and calibrated by GC. Conditions: an aqueous solution of CF_3SO_3H (initial pH 1.0, 3 mL) containing Ce^{IV} (1.67×10^{-1} M) and the catalyst (3.33×10^{-5} M).

lower TON than **3**. In comparison with complex **4**, the replacement of terpyridine with ligand L^{2-} gives complex **1** a TON that is 5.8 times higher than **4**, probably because the

Table 2. Rates of dioxygen evolution using Ce^{IV} as oxidant.

Complex	TON[a]	Rate[b]	Reference
1	553	2300,[c] 770[d]	this work
2	17	72,[c] 20[d]	this work
3	1170	340[d]	[33]
4	95	18[d]	[33]

[a] Measured with an oxygen sensor and calibrated by GC. [b] Initial rate in turnovers$^{-1} \times 10^4$. [c] A linear fitting of the initial curve was used to obtain the rate. [d] A second-order polynomial was used to fit the oxygen generated in first 60 min. The rate was calculated according to the slope of the curve at 30 min.

negatively charged ligand L^{2-} stabilizes the high-valent ruthenium intermediate and the small angle of O-Ru-O favors the formation of the seven-coordinated ruthenium intermediate.[30]

Kinetic study: The kinetic measurements were conducted by monitoring the decay of the absorbance of Ce^{IV} at 360 nm in an aqueous solution at pH 1.0 upon the addition of catalyst **1** or **2** (Figure 6). Under the given conditions, the decay of Ce^{IV} does not obey a simple exponential law. A linear dependence of the initial rate on either **1** or **2** is observed with
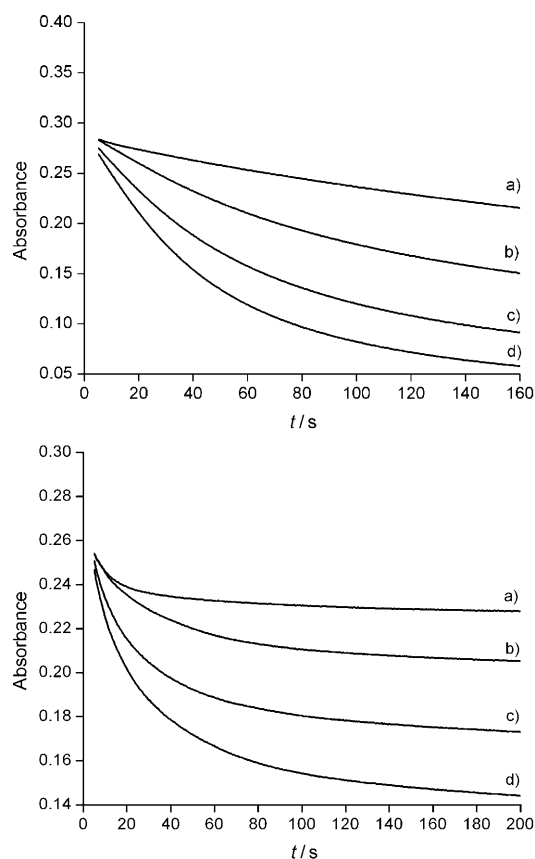

Figure 6. Monitoring of Ce^{IV} at 360 nm after the addition of complex **1** (0.5 (a), 2 (b), 4 (c), and 6 μM (d)) (upper) and complex **2** (2 (a), 4 (b), 6 (c), and 8 μM (d)) (lower) to an aqueous solution of Ce^{IV} (0.6 mM, pH 1.0). No data was collected in the first approximately 5 s due to the operation of injecting the catalyst and shaking the solution.

pseudo-first-order rate constants of 1.36 and 0.71 s^{-1}, respectively (Figure 7). Although these initial rate constants are of the same order of magnitude, the reaction system for **2** deactivates much faster than that for **1**, resulting in the low TON of **2** in water oxidation.
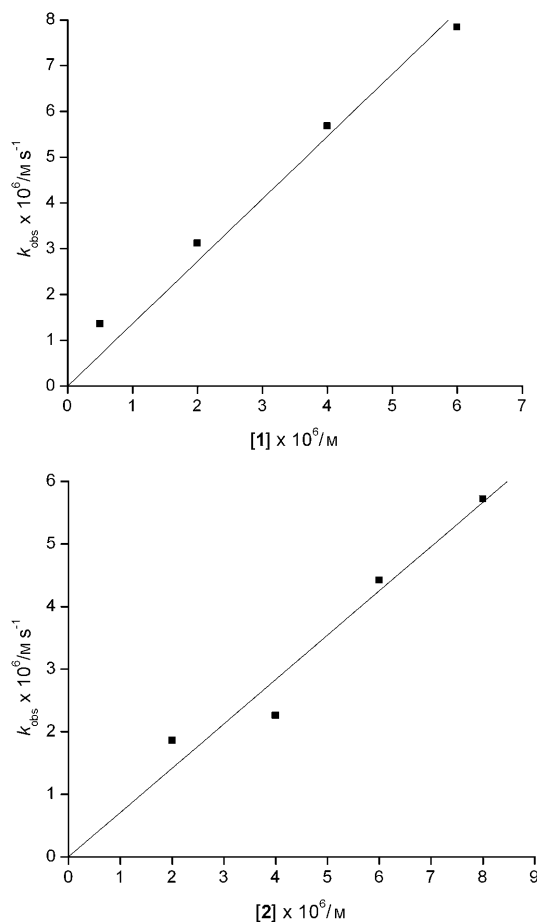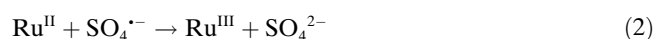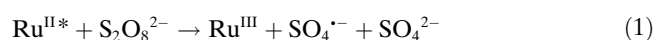

Figure 7. Upper: Plot of the initial rate (k_{obs}) versus concentration of complex **1**. The initial k_{obs} was calculated from the first 20 s of data shown in Figure 6, upper. The linear fit is shown by the line. $k_{obs} =$ 1.36 s^{-1}, $R = 0.999$. Lower: Plot of the initial rate (k_{obs}) versus concentration of complex **2**. The initial k_{obs} was calculated from the first 20 s of data shown in Figure 6, lower. The linear fit is shown by the line. $k_{obs} =$ 0.71 s^{-1}, $R = 0.972$.

Photochemical water oxidation: On the basis of the redox potential measurements, complexes **1** and **2** can catalyze the oxidation of water in pH 7.0 buffer at a lower potential than the reduction potential of [Ru(bpy)$_2$(dcb)]$^{3+}$. To generate [Ru(bpy)$_2$(dcb)]$^{3+}$ photochemically we chose Na$_2$S$_2$O$_8$ as a sacrificial electron acceptor to react with [Ru(bpy)$_2$(dcb)]$^{2+*}$ by oxidative quenching [Eq. (1)] and by a thermal reaction [Eq. (2)].[50]

$$Ru^{II}* + S_2O_8^{2-} \rightarrow Ru^{III} + SO_4^{\bullet-} + SO_4^{2-} \qquad (1)$$

$$Ru^{II} + SO_4^{\bullet-} \rightarrow Ru^{III} + SO_4^{2-} \qquad (2)$$

Photochemical water oxidation was conducted by using a three-component system composed of [Ru(bpy)$_2$(dcb)]$^{2+}$ as a photosensitizer, S$_2$O$_8^{2-}$ as a sacrificial electron acceptor, and a water oxidation catalyst (either **1** or **2**) (Figure 1). The light source was a 500 W xenon arc lamp equipped with a 400 nm cutoff filter and a water jacket to remove UV and IR radiation, respectively. The photo intensity produced was around 0.3 W cm^{-2}. All the photochemical reactions were maintained at around 11 °C. The kinetics of the photochemical water oxidation monitored by GC are depicted in Figure 8. Upon irradiation of the deoxygenated pH 7.2 phos-
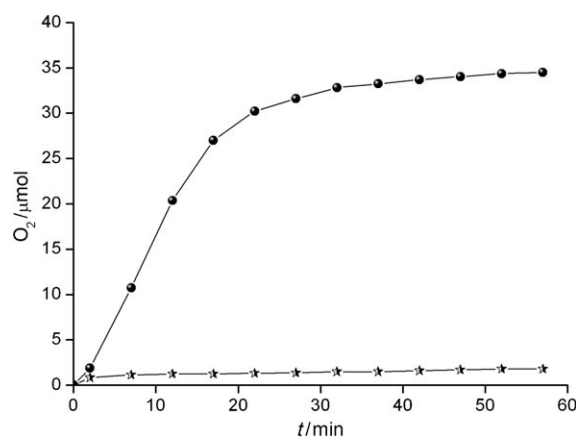

Figure 8. Photochemical oxygen evolution in 11.1 mL of a pH 7.2 phosphate buffer/acetonitrile (10:1.1, v/v) solution containing S$_2$O$_8^{2-}$ (9.0×10^{-3} M), [Ru(bpy)$_2$(dcb)]$^{2+}$ (5.0×10^{-4} M), and the catalyst (5.0×10^{-5} M). Complex **1** is shown by the circles and complex **2** is shown by the stars.

phate buffer solution containing [Ru(bpy)$_2$(dcb)]$^{2+}$, S$_2$O$_8^{2-}$, and complex **1**, oxygen was formed immediately and a maximum of around 34 μmol of oxygen was obtained after about 1 h of illumination, equivalent to a TON of 62 based on the catalyst. For complex **2**, the total dioxygen evolved was 2 μmol with a turnover of 3.7 based on the catalyst. Moreover, control experiments revealed that the oxygen generated in the above reaction was indeed promoted by our catalysts: 1) Under the same conditions but in the absence of the photosensitizer, no oxygen was generated during irradiation and 2) by using [RuCl$_3$·nH$_2$O] or [Ru(bpy)$_2$Cl$_2$] instead of a catalyst, no oxygen was detected after illumination of the triad system. These control experiments confirmed the ability of our catalysts to catalyze light-driven water oxidation.

MS analysis of the products of water oxidation: To obtain information on the reaction intermediates during the oxidation of water by **1** using Ce^{IV} as oxidant, we attempted to precipitate the products from the catalytic reaction.

The addition of 60 equiv of Ce^{IV} to a solution of complex **1** in a mixture of acetonitrile and a pH 1.0 aqueous solution (1:5, v/v) followed by the addition of an aqueous solution of NH$_4$PF$_6$ gave a blue precipitate. MS analysis of this blue

precipitate was carried out in acetonitrile (acn). Three complexes, $[Ru^{III}L(pic)_3]^+$, $[Ru^{III}L(pic)_2(acn)]^+$, and $[Ru^{III}L(pic)(acn)_2]^+$, were assigned, in agreement with the aforementioned 4-picoline dissociation. $[Ru^{III}L(pic)_2(acn)]^+$ and $[Ru^{III}L(pic)(acn)_2]^+$ were probably formed from $[Ru^{III}L(pic)_2(H_2O)]^+$ and $[Ru^{III}L(pic)(H_2O)_2]^+$, respectively, by ligand exchange with acetonitrile during the MS analysis measurements, which is a well-known reaction. Another fact contributing to this speculation is that dioxygen could be generated by the addition of solid complex **1** to an aqueous solution of Ce^{IV} (pH 1.0). Therefore, acetonitrile is not necessary for the catalytic activity. Our observations, combined with previous reports that several mononuclear ruthenium aqueous complexes efficiently catalyze the oxidation of water using Ce^{IV} as oxidant at pH 1.0,[30,31] strongly suggest that $[Ru^{III}L(pic)_2(H_2O)]^+$ is the real catalyst during the catalytic water oxidation by **1**. However, the ability of $[Ru^{III}L(pic)(H_2O)_2]^+$ to catalyze the water oxidation cannot be excluded.

Conclusion

We have synthesized and characterized two mononuclear ruthenium complexes (**1** and **2**) that have a negatively charged tridentate ligand, 2,6-pyridinedicarboxylate. Complex **1** shows high activity in Ce^{IV}-driven water oxidation with an initial turnover frequency of 0.23 turnovers^{-1}, which is one of the most active ruthenium-based water oxidation catalysts yet reported. Visible-light-driven water oxidation in a three-component system has been successfully demonstrated for both catalysts **1** and **2**, with a much higher efficiency of **1** compared with **2**. Complexes **1** and **2** are not stable in CH_3CN/H_2O and ligand exchange between acetonitrile and the carboxylate was observed. Protonation studies showed that it is the equatorial 4-picoline that is first released from complex **1** under acidic conditions. In addition, $[Ru^{III}L(pic)_3]$ undergoes ligand exchange between solvent (water or acetonitrile) and 4-picoline, which was proven by ^1H NMR spectroscopy by the formation of free 4-picoline. Accordingly, $[Ru^{III}L(pic)_2(H_2O)]^+$ is the most likely catalyst in the oxidation water with **1** as catalyst. These observations are important and useful for demonstrating the catalytic mechanistic aspects of those ruthenium catalysts structurally similar to **1**.

Experimental Section

General: $[Ru(dmso)_4Cl_2]$ and $[Ru(bpy)_2(dcb)]^{2+}$ were prepared according to literature methods.[51,52] All other chemicals were commercially available and all solvents were reagent grade. ^1H NMR spectra were recorded with a Bruker Avance 500 spectrometer. Mass spectrometry measurements were performed on a Q-Tof Micro mass spectrometer. IR spectra were obtained as KBr pellets on a Nicolet 21 spectrometer. Electronic absorption spectra of solutions in CH_3CN were measured with a CARY 300 Bio UV/Visible spectrophotometer. Elemental analyses were performed with a Thermoquest-Flash EA 1112 apparatus. Cyclic voltammet-

ric measurements were carried out with an Autolab potentiostat with a GPES electrochemical interface (Eco Chemie) using a glassy carbon disk (diameter 3 mm) as the working electrode and a platinum wire as the counter-electrode. The reference electrode was a nonaqueous Ag/Ag$^+$ electrode (0.1 M AgNO$_3$ in acetonitrile) for nonaqueous voltammetry or an Ag/AgCl electrode for aqueous voltammetry. The electrolytes used were either 0.1 M Bu$_4$NPF$_6$ in the corresponding organic solvents, an aqueous solution of CF$_3$SO$_3$H (pH 1.0) containing 10% acetonitrile, or pH 7.0 phosphate buffer (50 mM) containing 10% acetonitrile.

Irradiation: The photochemical evolution of oxygen was investigated under irradiation with a 500 W xenon arc lamp equipped with a 400 nm cut-off filter and a water jacket to remove UV and IR radiation, respectively. The photo intensity was around 0.3 Wcm^{-2}.

Oxygen evolution: Ce^{IV}-driven water oxidation was monitored by an oxygen sensor (Ocean Optics FOXY-OR125-G probe and Ocean Optics MFPF-100 fluorimeter) and calibrated by GC (a 3000A Micro GC (Agilent Technologies) equipped with a thermal conductive detector and a 5 Å molecular sieve column (12 μm/320 μm/10 m) and with helium as carrier gas). Typically, a 25 mL round flask was charged with a 1.67×10^{-1} M aqueous solution (aqueous solution of CF$_3$SO$_3$H, initial pH 1.0, 3 mL) of Ce^{IV} (the volume of the gas phase of the flask, excluding the space occupied by septa, oxygen sensor, and the solution, was 45 mL) and degassed by helium for 15 min (the background oxygen in the degassed system was measured by GC). Then the catalyst (100 μL, 1 mM) was injected and the evolution of dioxygen was monitored by the oxygen sensor and calibrated by GC at the end.

For photochemical oxygen generation, the reaction system was maintained at 11 °C by a circulating water-cooling system and the oxygen generated was measured by GC directly. In general, the three-component system of catalyst (5.0×10^{-5} M), sensitizer [Ru(bpy)$_2$(dcb)]$^{2+}$ (5×10^{-4} M), and electron acceptor S$_2$O$_8^{2-}$ (9×10^{-3} M) in pH 7.2 phosphate buffer/acetonitrile (10:1.1, v/v; total 11.1 mL) was degassed by helium for 15 min (the background was collected by GC) and then irradiated. After 2 min irradiation, the GC started sampling automatically every 5 min (the pump time is 10 s).

Synthesis of [RuL(pic)$_3$] (1): A mixture of H$_2$L (0.50 g, 3.0 mmol), [Ru(dmso)$_4$Cl$_2$] (1.45 g, 3.0 mmol), and NEt$_3$ (2.5 mL) in CH$_3$CN (25 mL) was degassed by N$_2$ and heated at reflux overnight. The color of this solution changed to dark-red from yellow. An excess of 4-picoline (4 mL) was added and the reflux was continued for an additional 4 h. The solvent was removed and the residues were washed with diethyl ether to eliminate the 4-picoline. The remaining oily part was dissolved in CH$_2$Cl$_2$ and washed with water to remove the triethylamine hydrochloric salt. The organic layer was dried over MgSO$_4$ overnight and the solvent was evaporated to afford the crude product. After purification by chromatography on Al$_2$O$_3$ with acetone/methanol (10:1, v/v), complex **1** was obtained as a dark-red solid (1.18 g, 72%). ^1H NMR (500 MHz, CDCl$_3$): $\delta = 8.75$ (d, $J = 6.5$ Hz, 2H), 8.12 (d, $J = 6.5$ Hz, 4H), 7.95 (d, $J = 8.0$ Hz, 2H), 7.54 (t, $J = 8.0$ Hz, 1H), 7.06 (d, $J = 6.0$ Hz, 2H), 6.86 (d, $J = 6.0$ Hz, 4H), 2.35 (s, 3H), 2.22 ppm (s, 6H); IR (KBr): $\nu_{max} = 1635$, 1618 cm^{-1} (C=O); UV/Vis (acetonitrile): λ_{max} $(\varepsilon) = 276$ (63794), 380 (14432), 453 nm (9150 dm^{3}mol^{-1}cm^{-1}); elemental analysis calcd (%) for C$_{25}$H$_{24}$N$_4$O$_4$Ru·2H$_2$O (581.58): C 51.63, H 4.85, N 9.63; found: C 51.89, H 4.72, N 9.41.

Synthesis of [RuL(bpy)(pic)] (2): A mixture of H$_2$L (167 mg, 1.0 mmol), [Ru(dmso)$_4$Cl$_2$] (484 mg, 1.0 mmol), and NEt$_3$ (0.8 mL) in CH$_3$CN (15 mL) was degassed by N$_2$ and heated at reflux overnight. A slight excess of 2,2'-bipyridine (169 mg, 1.08 mmol) was added and the reflux was continued for 4 h. Then 4-picoline (0.8 mL) was added and the mixture was heated at reflux overnight. A black solid precipitated from the solution. The solvent was removed and the residues were washed with diethyl ether to eliminate the 4-picoline. The remaining oily part was dissolved in CH$_2$Cl$_2$ and washed with water to remove the triethylamine hydrochloric salt. The organic layer was dried over MgSO$_4$ overnight and the solvent was evaporated to afford the crude product. After purification by chromatography on Al$_2$O$_3$ with dichloromethane/acetone (4:1, v/v), complex **2** was obtained as a dark-red solid (289 mg, 56%). ^1H NMR (500 MHz, CDCl$_3$): $\delta = 8.36$–8.27 (m, 4H), 8.19–8.153 (m, 3H), 7.86 (t, $J = $

7.5 Hz, 1H), 7.70 (t, $J = 7.5$ Hz, 1H), 7.63 (t, $J = 7.5$ Hz, 1H), 7.37–7.31 (m, 2H), 7.15–7.12 (m, 3H), 2.40 ppm (s, 3H); IR (KBr): $\nu_{max} = 1646$ cm^{-1} (C=O); UV/Vis (acetonitrile): λ_{max} (ε) = 292 (33045), 368 (7534), 430 (6259), 550 nm (3022 dm^{3}mol^{-1}cm^{-1}); elemental analysis calcd (%) for $C_{23}H_{18}N_4O_4Ru \cdot 2H_2O$ (551.51): C 53.59, H 3.52, N 10.87; found: C 53.41, H 3.56, N 10.52.

Crystal structure determinations: Suitable crystals of **1** were obtained by recrystallization from dichloromethane/hexane. Diffraction data were collected with a Bruker Nonius–KappaCCD diffractometer with Mo$_{K\alpha}$ radiation ($\lambda = 0.71073$ Å). Numerical absorption corrections were applied.[53] The structure was solved by direct methods and refined on $F2$ with anisotropic thermal parameters for all non-hydrogen atoms.[54] Proton atoms were refined on calculated positions using a riding model.

CCDC-747546 contains the supplementary crystallographic data for this paper. These data can be obtained free of charge from The Cambridge Crystallographic Data Centre via www.ccdc.cam.ac.uk/data_request/cif.

Crystallographic data for complex 1: Monoclinic, space group $P2_1/c$, $a = 16.021(1)$, $b = 23.715(3)$, $c = 14.531(1)$ Å, $\beta = 112.27(1)°$, $V = 5108.7(1)$ Å^3, $Z = 4$, $T = 293(2)$ K, $R_{all} = 0.1176$.

[1] K. N. Ferreira, T. M. Iverson, K. Maghlaoui, J. Barber, S. Iwata, *Science* **2004**, *303*, 1831–1838.

[2] N. Kamiya, J.-R. Shen, *Proc. Natl. Acad. Sci. USA* **2003**, *100*, 98–103.

[3] B. Loll, J. Kern, W. Saenger, A. Zouni, J. Biesiadka, *Nature* **2005**, *438*, 1040–1044.

[4] A. Zouni, H.-T. Witt, J. Kern, P. Fromme, N. Krauss, W. Saenger, P. Orth, *Nature* **2001**, *409*, 739–743.

[5] J. H. Alstrum-Acevedo, M. K. Brennaman, T. J. Meyer, *Inorg. Chem.* **2005**, *44*, 6802–6827.

[6] R. Eisenberg, H. Gray, *Inorg. Chem.* **2008**, *47*, 1697–1699.

[7] T. J. Meyer, *Acc. Chem. Res.* **1989**, *22*, 163–170.

[8] L. Sun, L. Hammarström, B. Åkermark, S. Styring, *Chem. Soc. Rev.* **2001**, *30*, 36–49.

[9] O. Khaselev, J. A. Turner, *Science* **1998**, *280*, 425–427.

[10] S. U. M. Khan, M. Al-Shahry, W. B. Ingler, Jr., *Science* **2002**, *297*, 2243–2245.

[11] A. Kudo, H. Kato, I. Tsuji, *Chem. Lett.* **2004**, *33*, 1534–1539.

[12] D. K. Zhong, J. Sun, H. Inumaru, D. R. Gamelin, *J. Am. Chem. Soc.* **2009**, *131*, 6086–6087.

[13] Z. Zou, J. Ye, K. Sayama, H. Arakawa, *Nature* **2001**, *414*, 625–627.

[14] K. Kalyanasundaram, M. Grätzel, *Angew. Chem.* **1979**, *91*, 759–760; *Angew. Chem. Int. Ed. Engl.* **1979**, *18*, 701–702.

[15] W. J. Youngblood, S.-H. A. Lee, Y. Kobayashi, E. A. Hernandez-Pagan, P. G. Hoertz, T. A. Moore, A. L. Moore, D. Gust, T. E. Mallouk, *J. Am. Chem. Soc.* **2009**, *131*, 926–927.

[16] R. Brimblecombe, G. F. Swiegers, G. C. Dismukes, L. Spiccia, *Angew. Chem.* **2008**, *120*, 7445–7448; *Angew. Chem. Int. Ed.* **2008**, *47*, 7335–7338.

[17] J. Limburg, J. S. Vrettos, L. M. Liable-Sands, A. L. Rheingold, R. H. Crabtree, G. W. Brudvig, *Science* **1999**, *283*, 1524–1527.

[18] A. K. Poulsen, A. Rompel, C. J. McKenzie, *Angew. Chem.* **2005**, *117*, 7076–7080; *Angew. Chem. Int. Ed.* **2005**, *44*, 6916–6920.

[19] M. Yagi, K. Narita, *J. Am. Chem. Soc.* **2004**, *126*, 8084–8085.

[20] M. Yagi, K. V. Wolf, P. J. Baesjou, S. L. Bernasek, G. C. Dismukes, *Angew. Chem.* **2001**, *113*, 3009–3012; *Angew. Chem. Int. Ed.* **2001**, *40*, 2925–2928.

[21] S. W. Gersten, G. J. Samuels, T. J. Meyer, *J. Am. Chem. Soc.* **1982**, *104*, 4029–4030.

[22] J. A. Gilbert, D. S. Eggleston, W. R. Murphy, D. A. Geselowitz, S. W. Gersten, D. J. Hodgson, T. J. Meyer, *J. Am. Chem. Soc.* **1985**, *107*, 3855–3864.

[23] Y. K. Lai, K. Y. Wong, *J. Electroanal. Chem.* **1995**, *380*, 193.

[24] M. K. Nazeeruddin, F. P. Rotzinger, P. Comte, M. Grätzel, *J. Chem. Soc. Chem. Commun.* **1988**, 872–874.

[25] H. H. Petach, M. Elliot, *J. Electrochem. Soc.* **1992**, *139*, 2217–2221.

[26] F. P. Rotzinger, S. Munavalli, P. Comte, J. K. Hurst, M. Graetzel, F. J. Pern, A. J. Frank, *J. Am. Chem. Soc.* **1987**, *109*, 6619–6626.

[27] M. Yagi, M. Kaneko, *Chem. Rev.* **2000**, *100*, 21–36.

[28] a) C. Sens, I. Romero, M. Rodriguez, A. Llobet, T. Parella, J. Benet-Buchholz, *J. Am. Chem. Soc.* **2004**, *126*, 7798–7799; b) F. Bozoglian, S. Romain, M. Z. Ertem, T. K. Todorova, C. Sens, J. Mola, M. Rodríguez, I. Romero, J. Benet-Buchholz, X. Fontrodona, C. J. Cramer, L. Gagliardi, A. Llobet, *J. Am. Chem. Soc.* **2009**, *131*, 15176–15187; c) J. Mola, E. Mas-Marza, X. Sala, I. Romero, M. Rodríguez, C. Viñas, T. Parella, A. Llobet, *Angew. Chem.* **2008**, *120*, 5914–5916; *Angew. Chem. Int. Ed.* **2008**, *47*, 5830–5832.

[29] a) T. Wada, K. Tsuge, K. Tanaka, *Inorg. Chem.* **2000**, *39*, 329–337; b) J. T. Muckerman, D. E. Polyansky, T. Wada, K. Tanaka, E. Fujita, *Inorg. Chem.* **2008**, *47*, 1787–1802.

[30] J. J. Concepcion, J. W. Jurss, J. L. Templeton, T. J. Meyer, *J. Am. Chem. Soc.* **2008**, *130*, 16462–16463.

[31] a) S. Masaoka, K. Sakai, *Chem. Lett.* **2009**, *38*, 182–183; b) M. Yoshida, S. Masaoka, K. Sakai, *Chem. Lett.* **2009**, *38*, 702–703.

[32] Z. Deng, H.-W. Tseng, R. Zong, D. Wang, R. Thummel, *Inorg. Chem.* **2008**, *47*, 1835–1848.

[33] H.-W. Tseng, R. Zong, J. T. Muckerman, R. Thummel, *Inorg. Chem.* **2008**, *47*, 11763–11773.

[34] G. Zhang, R. Zong, H.-W. Tseng, R. P. Thummel, *Inorg. Chem.* **2008**, *47*, 990–998.

[35] R. Zong, R. P. Thummel, *J. Am. Chem. Soc.* **2005**, *127*, 12802–12803.

[36] Y. V. Geletii, B. Botar, P. Kögerler, D. A. Hillesheim, D. G. Musaev, C. L. Hill, *Angew. Chem.* **2008**, *120*, 3960–3963; *Angew. Chem. Int. Ed.* **2008**, *47*, 3896–3899.

[37] A. Sartorel, M. Carraro, G. Scorrano, R. D. Zorzi, S. Geremia, N. D. McDaniel, S. Bernhard, M. Bonchio, *J. Am. Chem. Soc.* **2008**, *130*, 5006–5007.

[38] N. D. McDaniel, F. J. Coughlin, L. L. Tinker, S. Bernhard, *J. Am. Chem. Soc.* **2008**, *130*, 210–217.

[39] J. F. Hull, D. Balcells, J. D. Blakemore, C. D. Incarvito, O. Eisenstein, G. W. Brudvig, R. H. Crabtree, *J. Am. Chem. Soc.* **2009**, *131*, 8730–8731.

[40] J. L. Cape, J. K. Hurst, *J. Am. Chem. Soc.* **2008**, *130*, 827–829.

[41] P. Comte, M. K. Nazeeruddin, F. P. Rotzinger, A. J. Frank, M. Grätzel, *J. Mol. Catal.* **1989**, *52*, 63–84.

[42] Y. V. Geletii, Z. Huang, Y. Hou, D. G. Musaev, T. Lian, C. L. Hill, *J. Am. Chem. Soc.* **2009**, *131*, 7522–7523.

[43] L. Duan, Y. Xu, P. Zhang, M. Wang, L. Sun, *Inorg. Chem.* **2010**, *49*, 209–215.

[44] Y. Xu, L. Duan, L. Tong, B. Åkermark, L. Sun, unpublished results.

[45] A. Harriman, G. Porter, P. Walters, *J. Chem. Soc. Faraday Trans. 2* **1981**, *77*, 2373–2383.

[46] S. W. Kohl, L. Weiner, L. Schwartsburd, L. Konstantinovski, L. J. W. Shimon, Y. Ben-David, M. A. Iron, D. Milstein, *Science* **2009**, *324*, 74–77.

[47] Y. Xu, T. Åkermark, V. Gyollai, D. Zou, L. Eriksson, L. Duan, R. Zhang, B. Åkermark, L. Sun, *Inorg. Chem.* **2009**, *48*, 2717–2719.

[48] L. Duan, A. Fischer, Y. Xu, L. Sun, *J. Am. Chem. Soc.* **2009**, *131*, 10397–10399.

[49] N. G. Connelly, W. E. Geiger, *Chem. Rev.* **1996**, *96*, 877–910.

[50] K. Henbest, P. Douglas, M. S. Garley, A. Mills, *J. Photochem. Photobiol. A* **1994**, *80*, 299–305.

[51] E. Dulière, M. Devillers, J. Marchand-Brynaert, *Organometallics* **2003**, *22*, 804–811.

[52] C. M. Elliott, E. J. Hershenhart, *J. Am. Chem. Soc.* **2002**, *124*, 7519–7526.

[53] HABITUS, A program for numerical absorption correction, H. B. W. Herrendorf, Universities of Giessen and Karlsruhe, Germany, **1997**.

[54] SHELXL97, A program for crystal structure refinement, G. S. Sheldrick, University of Göttingen, Göttingen, **1997**.

 © 2010 Wiley-VCH Verlag GmbH & Co. KGaA, Weinheim